

11-5-2001

# Characterization of the native $\text{Cr}_2\text{O}_3$ oxide surface of $\text{CrO}_2$

Ruihua Cheng  
*University of Nebraska-Lincoln*

B. Xu  
*University of Nebraska-Lincoln*

C.N. Borca  
*University of Nebraska-Lincoln*

Andrei Sokolov  
*University of Nebraska-Lincoln, sokolov@unl.edu*

C.S. Yang  
*University of Nebraska-Lincoln*

*See next page for additional authors*

Follow this and additional works at: <http://digitalcommons.unl.edu/physicsdowben>

 Part of the [Physics Commons](#)

---

Cheng, Ruihua; Xu, B.; Borca, C.N.; Sokolov, Andrei; Yang, C.S.; Yuan, Lu; Liou, Sy\_Hwang; Doudin, Bernard; and Dowben, Peter A., "Characterization of the native  $\text{Cr}_2\text{O}_3$  oxide surface of  $\text{CrO}_2$ " (2001). *Peter Dowben Publications*. 22.  
<http://digitalcommons.unl.edu/physicsdowben/22>

This Article is brought to you for free and open access by the Research Papers in Physics and Astronomy at DigitalCommons@University of Nebraska - Lincoln. It has been accepted for inclusion in Peter Dowben Publications by an authorized administrator of DigitalCommons@University of Nebraska - Lincoln.

---

**Authors**

Ruihua Cheng, B. Xu, C.N. Borca, Andrei Sokolov, C.S. Yang, Lu Yuan, Sy\_Hwang Liou, Bernard Doudin, and Peter A. Dowben

## Characterization of the native $\text{Cr}_2\text{O}_3$ oxide surface of $\text{CrO}_2$

Ruihua Cheng, B. Xu, C. N. Borca, A. Sokolov, C. -S. Yang, L. Yuan, S. -H. Liou, B. Doudin, and P. A. Dowben<sup>a)</sup>

*Department of Physics and Astronomy and the Center for Materials Research and Analysis (CMRA), Behlen Laboratory of Physics, University of Nebraska—Lincoln Lincoln, Nebraska 68588-0111*

(Received 5 July 2001; accepted for publication 29 August 2001)

Using photoemission and inverse photoemission, we have been able to characterize the  $\text{Cr}_2\text{O}_3$  oxide surface of  $\text{CrO}_2$  thin films. The  $\text{Cr}_2\text{O}_3$  surface oxide exhibits a band gap of about 3 eV, although the bulk  $\text{CrO}_2$  is conducting. The thickness of this insulating  $\text{Cr}_2\text{O}_3$  layer is twice the photoelectron escape depth which is about 2 nm thick. The effective  $\text{Cr}_2\text{O}_3$  surface layer Debye temperature, describing motion normal to the surface, is about 370 K. From a comparison of  $\text{CrO}_2$  films grown by different techniques, with different  $\text{Cr}_2\text{O}_3$  content, evidence is provided that the  $\text{CrO}_2$  may polarize the  $\text{Cr}_2\text{O}_3$ . © 2001 American Institute of Physics. [DOI: 10.1063/1.1416474]

Among the predicted half-metallic ferromagnets (metallic for one spin direction while insulating for the other spin direction, i.e., 100% spin polarization),  $\text{CrO}_2$  routinely exhibits the highest polarization but among the lowest tunnel magnetoresistance. With half-metallic character expected on the basis of theory,<sup>1–6</sup> very large tunneling magnetoresistance (TMR) is expected<sup>7–9</sup> (ideally the TMR between two half-metallic ferromagnets should be infinite), but a much smaller (1%) magnetoresistance was found on  $\text{CrO}_2$  tunnel junctions at 70 K.<sup>10</sup> Evidence of 90% to 100% polarization has been, however, observed in spin-polarized photoemission,<sup>11</sup> vacuum tunneling,<sup>12</sup> and Andreev scattering.<sup>13–15</sup> This work addresses the surface composition and properties of  $\text{CrO}_2$  thin films, going beyond the simple confirmation that the stable oxide surface of  $\text{CrO}_2$  is  $\text{Cr}_2\text{O}_3$ .<sup>16</sup>

We investigated the surfaces of  $\text{CrO}_2$  films fabricated by two different techniques. One class of films were fabricated by laser initiated organometallic chemical vapor deposition (OMCVD),<sup>17</sup> while the other type of films were made by rf sputtering of  $\text{CrO}_3$  onto  $\text{LaAlO}_3$  substrates and annealing in a high-pressure cell.<sup>18</sup> Annealing in about 100 atm of oxygen pressure at 390 °C leads to a stable  $\text{CrO}_2$  phase.

Prior to our studies, samples were cleaned by sputtering and annealing to remove surface contamination. From the outset, i.e., from the initial stages of surface preparation, the core level binding energies indicated that the stable surfaces were  $\text{Cr}_2\text{O}_3$ . X-ray photoemission spectroscopy (XPS) measurements were obtained using the  $\text{Mg } K_\alpha$  line radiation (1253.6 eV) and the photoemission (UPS) measurements were acquired about normal emission angle using the He I line (21.2 eV). The inverse photoemission IPES spectra were obtained by using variable energy electrons (from 5 to 19 eV) at normal incidence and a Geiger–Muller UV photodetector. The energy resolution was  $\sim 450$  meV in inverse photoemission. For both photoemission and inverse photoemission, the Fermi level was established from tantalum in electrical contact with the sample.

Figure 1 shows the room temperature normal emission

photoemission data of both the Cr 2*p* and O 1*s* core levels for both sputter deposited and laser assisted OMCVD deposited  $\text{CrO}_2$  thin film samples. The binding energy of Cr 2*p*<sub>3/2</sub> core level for the laser assisted OMCVD deposited  $\text{CrO}_2$  thin film samples is about  $576.8 \pm 0.2$  eV which generally corresponds to the accepted binding energy for  $\text{Cr}_2\text{O}_3$  oxide.<sup>19</sup> The Cr 2*p*<sub>3/2</sub> for the sputtered samples are somewhat lower, at about  $576.3 \pm 0.3$  eV. This suggests that the sputtered samples are more dominated by the  $\text{CrO}_2$  oxide<sup>20</sup> in the surface region, though a shoulder at around 576.8 eV binding energy indicates the presence of some  $\text{Cr}_2\text{O}_3$ . The presence of both  $\text{CrO}_2$  and  $\text{Cr}_2\text{O}_3$  oxide phases in the surface region of the sputter deposited samples is more apparent in the oxygen core level spectra.

The binding energy of O 1*s* core level for OMCVD deposited sample is  $531.1 \pm 0.2$  eV and the spectrum for the sputtered sample also shows the peak at  $531.1 \pm 0.2$  eV as well as a significant shoulder around  $529.5 \pm 0.2$  eV. This suggests that the surfaces of both samples contain  $\text{Cr}_2\text{O}_3$ , but the  $\text{Cr}_2\text{O}_3$  layer on the surface of sputtered films are thinner than the case for the OMCVD films. This conclusion is supported by the angle-resolved XPS (ARXPS) data in Fig. 2.

We used ARXPS to characterize the thickness of the  $\text{Cr}_2\text{O}_3$  surface layer for the sputter deposited  $\text{CrO}_2$  films, as has been undertaken for other oxide surfaces.<sup>21</sup> The ratio of the  $\text{Cr}_2\text{O}_3$  intensity to the  $\text{CrO}_2$  intensity for each emission angle was derived by decomposing every O 1*s* spectrum into two peaks, corresponding to the  $\text{Cr}_2\text{O}_3$  and  $\text{CrO}_2$  oxide phases, respectively. This intensity ratio is shown in Fig. 2. Since the  $\text{Cr}_2\text{O}_3$  signal increases relative to the  $\text{CrO}_2$  signal at the higher emission angles, it is clear that  $\text{Cr}_2\text{O}_3$  dominates the surface as the effective probing depth decreases with increasing emission angle. We find that the thickness of  $\text{Cr}_2\text{O}_3$  layer is about twice the oxygen core level photoelectron mean free path, using a summation modeling analysis described elsewhere.<sup>21</sup> This corresponds to approximately 2 nm thickness. Thus, while the x-ray diffraction data, shown as the inset in Fig. 2, is dominated by significant  $\text{CrO}_2$  peaks, there is a small amount of the  $\text{Cr}_2\text{O}_3$  signal, which probably has some contributions from the  $\text{Cr}_2\text{O}_3$  surface of the sample. For the OMCVD deposited films, the  $\text{Cr}_2\text{O}_3$  surface oxide is much thicker than the electron mean free path and therefore

<sup>a)</sup>Author to whom all correspondence should be addressed at: Department of Physics and Astronomy, 255 Behlen Laboratory of Physics, University of Nebraska, Lincoln, Nebraska 68588-0111; electronic mail: pdowben@unl.edu

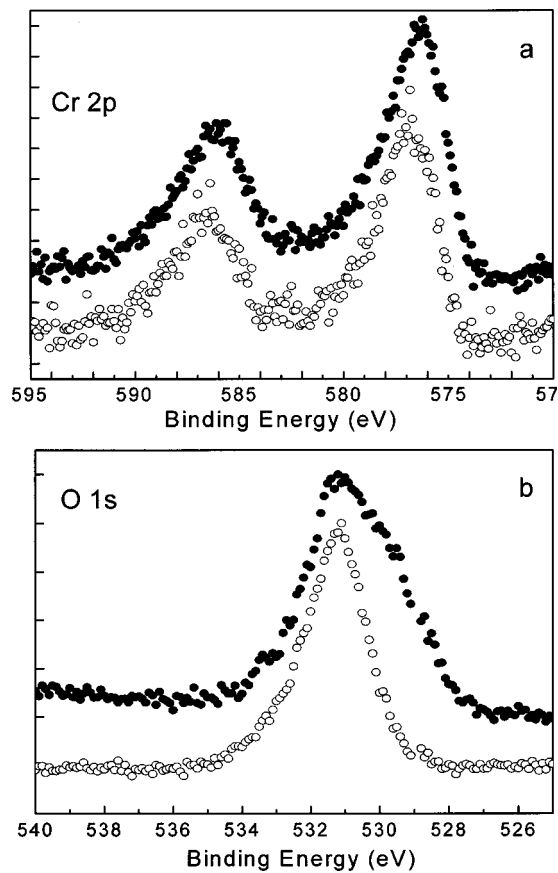


FIG. 1. Upper panel shows the XPS core level photoemission of Cr  $2p$  at room temperature. Lower panel shows the O  $1s$  photoemission data at room temperature. The sample fabricated by OMCVD is shown as open circles and the sample fabricated by sputtering is shown as closed circles.

is much thicker than is the case for the sputter deposited films.

The combined valence band photoemission (UPS) and inverse photoemission data taken at room temperature is shown in Fig. 3 for the sputter deposited film (curve B). A large band gap of  $E_g = 2.8$  eV (at room temperature) is evident between valence band and conductance band edges. The gap is much bigger than  $3$  kT, which is a clear indication that the surface of  $\text{CrO}_2$  is insulating, not conducting.

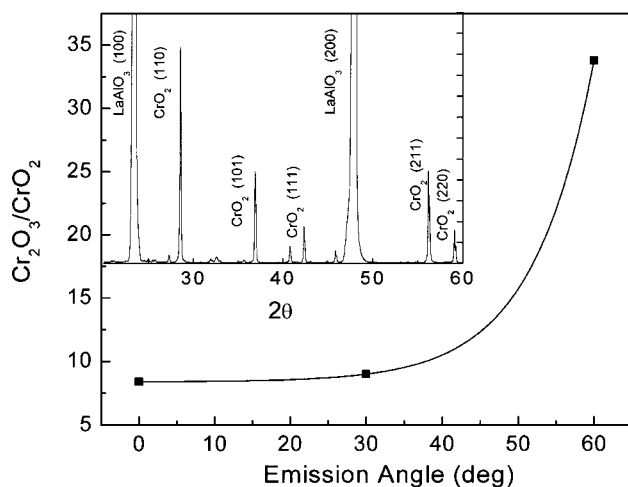


FIG. 2. The room temperature XPS intensity ratio of  $\text{Cr}_2\text{O}_3$  peak to  $\text{CrO}_2$  peak vs different emission angle for sputter deposited films. The x-ray diffraction data of the sample is shown in the inset.

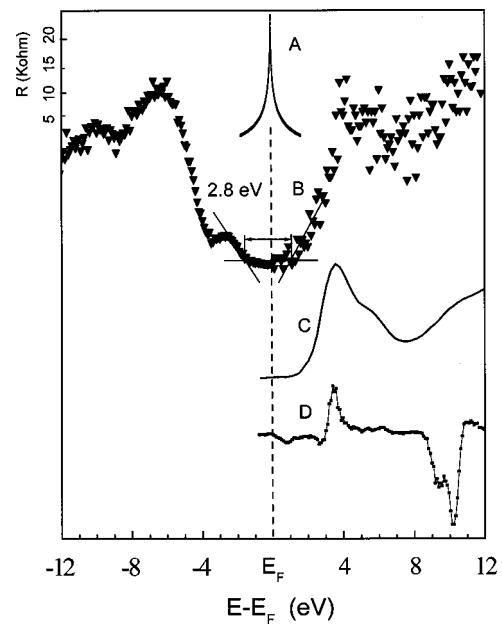


FIG. 3. A comparison of the density of states in the region of the Fermi level from resistivity (transport measurements) of the sputter deposited film at  $1.52$  K (a), the combined photoemission (UPS) and the inverse photoemission (IPES) at room temperature for the sputter deposited films (b), X-ray adsorption at the O  $1s$  level (c) together with the Cr  $2p_{3/2}$  edge MCD spectra (d), were both aligned using the core level binding energies for  $\text{CrO}_2$ . Spectra C and D were taken of the OMCVD deposited sample dominated by significant amounts of  $\text{Cr}_2\text{O}_3$  while the inverse photoemission and resistivity data were taken from a sputter deposited sample. Spectra B–D were taken at room temperature.

The transport measurements, at  $1.52$  K, showing the resistance at low bias voltages in the sputter deposited film, are shown in curve A of Fig. 3. At low temperatures, the resistance between  $\text{CrO}_2$  grains in the bulk of the thin film shows a dramatic increase only near zero bias. This, together with the absence of significant surface photocharging down to  $170$  K, suggests that there are conduction paths through the surface region and intergrain  $\text{Cr}_2\text{O}_3$  layers. Thus, while there is little evidence of conduction path or defects states within a volt of the Fermi level, such states must exist, though perhaps much less than  $2\%$ – $3\%$  of the  $\text{Cr}_2\text{O}_3$  layers. This is consistent with the evidence of Coulomb blockade<sup>18</sup> that also suggests that the  $\text{Cr}_2\text{O}_3$  oxide surface of  $\text{CrO}_2$  crystallites is imperfect and contains defects. For OMCVD samples, we do not find any such conducting paths, but the  $\text{Cr}_2\text{O}_3$  content is higher in these latter films.

In Fig. 3, we lined up the chromium  $L_3(2p_{3/2})$  edge magnetic circular dichroism (MCD) signal, and O  $1s$  x-ray adsorption (XAS) spectra with the Fermi energy, based on the chromium and oxygen XPS binding energies for an OMCVD sample (characterized by significant  $\text{Cr}_2\text{O}_3$  inclusions in the  $\text{CrO}_2$ .<sup>17</sup>) The O  $1s$  XAS edge spectrum (curve C in Fig. 3) is consistent with a  $\text{Cr}_2\text{O}_3$  phase<sup>22</sup> dominant in the surface region of the thin film material. The MCD results, shown as plot D in Fig. 3, provide indications of magnetic ordering in the unoccupied bands at the  $L_3$  chromium edge. Nonetheless, at the onset in the MCD signal at the threshold, the magnetic ordering of the states close to the Fermi level appears to be dominated by spin minority (curve D in Fig. 3), which is inconsistent with the half-metallic character or even high spin polarization predicted for  $\text{CrO}_2$ .<sup>2–6</sup> The recognition

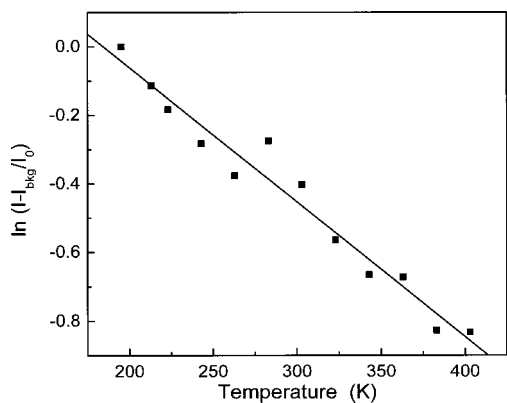


FIG. 4. The logarithm of XPS intensity of Cr  $2p_{3/2}$  core level vs temperature. The fit expected for an effective Debye temperature of 370 K is shown.

that the surfaces of  $\text{CrO}_2$  films are  $\text{Cr}_2\text{O}_3$  (Ref. 16) does much to explain the very low density of states near the Fermi energy in the spin-polarized photoemission measurements,<sup>11</sup> but fails to explain the high polarization asymmetry observed in spin-polarized photoemission.<sup>11</sup> Induced polarization of the thin  $\text{Cr}_2\text{O}_3$  surface layer, perhaps enhanced by defects, is clearly necessary to explain values of polarization approaching 90% to 100% reported in spin-polarized photoemission,<sup>11</sup> that in hindsight may be dominated by a  $\text{Cr}_2\text{O}_3$  surface layer. While the x-ray diffraction results presented herein and elsewhere<sup>23</sup> suggest that the  $\text{Cr}_2\text{O}_3$  surface layer is the anti-ferromagnetic corundum structure, the gamma, or cubic spinel structures of  $\text{Cr}_2\text{O}_3$  that can show considerable stability at the surface,<sup>24</sup> can not be excluded as the dominant structure, and might more easily polarize the generally more stable corundum structure. Such an explanation is consistent with the results presented here.

The effective surface Debye temperature of the  $\text{Cr}_2\text{O}_3$  surface layer can be evaluated by XPS and other surface sensitive techniques such as low-energy electron diffraction and reflection high-energy electron diffraction.<sup>25</sup> In the absence of surface phase transition, it is assumed that the emerging electron-beam intensity depends exponentially upon the sample temperature and this dependence is applicable to core level XPS at normal emission angle. The intensity of the photoelectron peak can be written as

$$I = I_0 \exp[-2W(T)], \quad \text{with } 2W = \frac{3\hbar^2(\Delta k)^2 T}{mk_B \theta_D^2},$$

where  $W$  is the Debye–Waller factor,  $T$  is the sample temperature,  $\hbar(\Delta k)$  is the electron momentum transfer,  $m$  is the mass of the scattering center, and  $\theta_D$  is the effective surface Debye temperature. The effective Debye temperature can be evaluated from the slope of a plot of  $\ln(I/I_0)$  as a function of sample temperature, as shown in Fig. 4. A linear background was subtracted from each spectrum and normalization with respect to the intensity at the lowest temperature ( $I_0$ ). We find that the effective Debye temperature  $\theta_D$  is about 370 K. While typical of a metal, this effective Debye temperature is rather low for an oxide insulator and might contribute to strong temperature effects in Coulomb blockade.<sup>18</sup>

We have investigated  $\text{CrO}_2$  thin film surfaces by using both x-ray photoemission and inverse photoemission. Our data show a large band gap between valence and conduction

bands, which indicates that the surface of  $\text{CrO}_2$  film is insulating, while the transport measurements show that bulk material is conducting. We identify  $\text{Cr}_2\text{O}_3$  as a stable oxide surface on  $\text{CrO}_2$  films with an effective surface Debye temperature of about 370 K for the  $\text{Cr}_2\text{O}_3$  surface layer. From ARXPS data, we found that the thickness of this insulating  $\text{Cr}_2\text{O}_3$  layer is two times the mean free path. The  $\text{CrO}_2$  “bulk” may induce some polarization in the  $\text{Cr}_2\text{O}_3$  surface layer.

The support of the NSF (DMR 98-02126), the NSF CAREER program (Grant No. DMR 98-74657), the Office of Naval Research, and the Nebraska Research Initiative are gratefully acknowledged.

- <sup>1</sup>J. B. Goodenough, in *Progress in Solid State Chemistry*, edited by H. Reiss (Pergamon, Oxford, 1971), Vol. 5, p. 145.
- <sup>2</sup>H. van Lueken and R. A. de Groot, *Phys. Rev. B* **51**, 7176 (1995).
- <sup>3</sup>K. Schwarz, *J. Phys. F: Met. Phys.* **16**, L211 (1986).
- <sup>4</sup>S. Matar, G. Demazeau, J. Sticht, V. Eyert, and J. Kübler, *J. de Physique I* **2**, 315 (1992).
- <sup>5</sup>M. A. Korotin, V. I. Anisimov, D. I. Khomskii, and G. A. Sawatzky, *Phys. Rev. Lett.* **80**, 4305 (1998).
- <sup>6</sup>S. P. Lewis, P. B. Allen, and T. Sasaki, *Phys. Rev. B* **55**, 10253 (1997).
- <sup>7</sup>H. Y. Hwang and S.-W. Cheong, *Science* **278**, 1607 (1997).
- <sup>8</sup>K. Suzuki and P. M. Tedrow, *Phys. Rev. B* **58**, 11597 (1998); A. M. Bratkovsky, *Phys. Rev. B* **56**, 2344 (1997).
- <sup>9</sup>S. S. Manoharan, D. Elefant, G. Reiss, and J. B. Goodenough, *Appl. Phys. Lett.* **72**, 984 (1998).
- <sup>10</sup>A. Barry, J. M. D. Coey, and M. Viret, *J. Phys.: Condens. Matter* **12**, L173 (2000).
- <sup>11</sup>K. P. Kämper, W. Schmitt, G. Güntherodt, R. J. Gambino, and R. Ruf, *Phys. Rev. Lett.* **59**, 2788 (1987).
- <sup>12</sup>R. Weisendanger, H.-J. Güntherodt, G. Güntherodt, R. J. Gambino, and R. Ruf, *Phys. Rev. Lett.* **65**, 247 (1990).
- <sup>13</sup>R. J. Soulen, J. M. Byers, B. Nadgorny, T. Ambrose, S. F. Cheng, P. R. Broussard, C. T. Tanaka, J. Nowak, J. S. Moodera, A. Barry, and J. M. D. Coey, *Science* **282**, 85 (1998).
- <sup>14</sup>R. J. Soulen, M. S. Osofsky, B. Nadgorny, T. Ambrose, P. Broussard, and S. F. Cheng, *J. Appl. Phys.* **85**, 4589 (1999).
- <sup>15</sup>W. J. DeSisto, P. R. Broussard, T. F. Ambrose, B. E. Nadgorny, and M. S. Osofsky, *Appl. Phys. Lett.* **76**, 3789 (2000).
- <sup>16</sup>J. Dai, J. Tang, H. Xu, L. Spinu, W. Wang, K.-Y. Wang, A. Kumbhar, M. Li, and U. Diebold, *Appl. Phys. Lett.* **77**, 2840 (2000).
- <sup>17</sup>P. A. Dowben, Y.-G. Kim, S. Baral-Tosh, G. O. Ramseyer, C. Hwang, and M. Onellion, *J. Appl. Phys.* **67**, 5658 (1990); R. Cheng, C. N. Borca, and P. A. Dowben, *Mater. Res. Soc. Symp. Proc.* **614**, F10.4.1 (2000).
- <sup>18</sup>A. Sokolov, C.-S. Yang, L. Yuan, S.-H. Liou, R. Cheng, B. Xu, C. N. Borca, P. A. Dowben and B. Doubin (unpublished).
- <sup>19</sup>C. Battistoni, J. L. Dormann, D. Fiorani, E. Paparazzo, and S. Viticoli, *Solid State Commun.* **39**, 581 (1981).
- <sup>20</sup>I. Ikemoto, K. Ishii, S. Kinoshita, H. Kuroda, M. A. A. Franco, and J. Thomas, *J. Solid State Chem.* **17**, 425 (1976).
- <sup>21</sup>J. Choi, J. Zhang, S.-H. Liou, P. A. Dowben, and E. W. Plummer, *Phys. Rev. B* **59**, 13453 (1999); H. Dulli, E. W. Plummer, P. A. Dowben, Jaewu Choi, and S.-H. Liou, *Appl. Phys. Lett.* **77**, 570 (2000); Hani Dulli, P. A. Dowben, S.-H. Liou, and E. W. Plummer, *Phys. Rev. B* **62**, R14629 (2000); C. N. Borca, Bo Xu, T. Komesu, H.-Ky. Jeong, M. T. Liu, S.-H. Liou, and P. A. Dowben, *Appl. Phys. Lett.* (submitted).
- <sup>22</sup>C. B. Stagaescu, X. Su, D. E. Eastman, K. N. Altmann, F. J. Himpsel, and A. Gupta, *Phys. Rev. B* **61**, R9233 (2000).
- <sup>23</sup>R.-H. Cheng, C. N. Borca, P. A. Dowben, S. Stadler, and Y. U. Idzerda, *Appl. Phys. Lett.* **78**, 521 (2001); J. Graham, *J. Phys. Chem. Solids* **17**, 18 (1960).
- <sup>24</sup>P. S. Robert, H. Geisler, C. A. Ventrice, J. van Ek, S. Chaturvedi, J. A. Rodriguez, M. Kuhn, and U. Diebold, *J. Vac. Sci. Technol. A* **16**, 990 (1998).
- <sup>25</sup>C. Waldfried, D. N. McIlroy, J. Zang, P. A. Dowben, G. A. Katrich, and E. W. Plummer, *Surf. Sci.* **363**, 296 (1996); C. N. Borca, D. Ristoiu, T. Komesu, H.-K. Jeong, C. Hordequin, J. Pierre, J. P. Nozieres, and P. A. Dowben, *Appl. Phys. Lett.* **77**, 88 (2000).